

Propagation of weakly nonlinear waves in stratified media having mixed nonlinearity

By A. KLUWICK¹ AND E. A. COX²

¹Institute of Fluid Dynamics and Heat Transfer, Technical University, Vienna

²Department of Mathematical Physics, University College Dublin, Dublin 4, Ireland

(Received 6 November 1991 and in revised form 25 April 1992)

The evolution of small-amplitude finite-rate waves in fluids having high specific heats is studied adopting the assumption that the unperturbed state varies in the propagation direction. It is shown that this not only leads to quantitative changes of the results holding for homogeneous media but also gives rise to new phenomena. Most interesting, shocks are found to terminate at a finite distance from the origin if the fundamental derivative changes sign along the propagation path.

1. Introduction

Recent theoretical and experimental studies indicate that fluids with high specific heats may prove useful in a number of technological applications including problems on nonlinear acoustics, steady and unsteady internal flows, viscous–inviscid interactions, flows with phase changes, etc. Apart from being of importance as far as future applications are concerned, investigations dealing with such fluids are also of interest in their own right. In fact they have revealed a surprising richness of new phenomena even if the considerations are restricted to the case of single-phase fluids. Expansion shocks provide a prominent example of such new phenomena, which were previously thought impossible.

In the limit of small-amplitude disturbances the answer to the question of whether compression shocks or expansion shocks may form in a fluid depends solely on the sign of the so-called fundamental derivative

$$\Gamma(\tilde{\rho}, \tilde{s}) = \frac{1}{\tilde{a}} \left. \frac{\partial(\tilde{a}\tilde{\rho})}{\partial\tilde{\rho}} \right|_{\tilde{s}} \quad (1.1)$$

introduced by Hayes (1960). Here

$$\tilde{a}(\tilde{\rho}, \tilde{s}) = \left(\frac{\partial\tilde{p}}{\partial\tilde{\rho}} \right)_{\tilde{s}}^{\frac{1}{2}} \quad (1.2)$$

is the local sound speed and $\tilde{\rho}$, \tilde{p} , \tilde{s} are the local fluid density, pressure and entropy; dimensional quantities will be denoted by \sim throughout.

If the fluid has $\Gamma > 0$ the propagation speed of wavelets increases with the excess pressure and the associated nonlinear steepening of the wave profile will therefore lead to the occurrence of compression shocks only. An example of a strictly positive Γ is the perfect gas and, consequently, the perfect gas admits only compression shocks. In contrast, if $\Gamma < 0$ wavelets carrying lower values of the excess pressure travel faster than those carrying higher values and expansion shocks are thus found to be the only jump discontinuities capable of propagating through the fluid. The

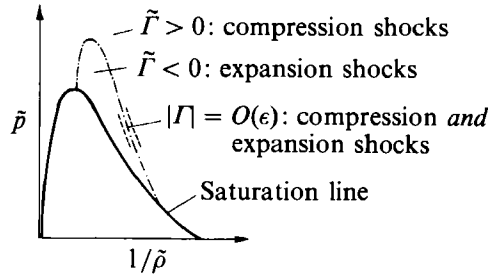


FIGURE 1. Regions of $\Gamma > 0$ and $\Gamma < 0$ in the $(\bar{p}, 1/\bar{\rho})$ -plane.

first theoretical studies which point to the existence of this type of fluid have been carried out by Bethe (1942) and independently by Zel'dovich (1946) who showed that Van der Waals gases exhibit regions with $\Gamma < 0$ near the critical point provided the specific heats are sufficiently high, $c_v/R > 17$. Here c_v and R denote the specific heat at constant volume and the gas constant, respectively. An important further step was taken by Thompson & Lambrakis (1973). Using the Van der Waals equation as well as more refined constitutive relations, they were able to give the first specific examples of real fluids having $\Gamma < 0$, which include hydrocarbons and fluorocarbons of moderate complexity. Most recently, a detailed study of the thermodynamic properties of fluorocarbons has been carried out by Cramer (1991) who applied the Martin Hou equation to calculate Γ . Each of the seven commercially available fluorocarbons was found to exhibit a region of $\Gamma < 0$ large enough to include the critical isotherm.

According to the theoretical studies cited so far the fundamental derivative Γ can, in fact, change sign for a class of single phase fluids. Following a proposal of Cramer (1991) such fluids will be termed Bethe–Zel'dovich–Thompson (BZT) fluids in recognition of the pioneering contributions made by those scholars of real-fluid effects. Nevertheless, it should be noted that the existence of such fluids has still to be verified experimentally, for example, by generating a single-phase expansion shock. Experiments, which show the formation of expansion shocks in Freon-13 have been carried out by Borisov *et al.* (1983) Unfortunately, however, the flow appears to have also entered the two-phase region.

Although the experimental detection of a single expansion shock would certainly represent a spectacular event from a physical point of view the mathematical theory which describes the properties of such shocks is much less spectacular. In fact, in the limit of weak shocks the effect of negative nonlinearity can be incorporated quite easily into the classical theory of nonlinear acoustics. The situation changes drastically, however, if the unperturbed state of the BZT fluid is sufficiently close to the $\Gamma = 0$ curve relative to the wave amplitude (see figure 1). Even small disturbances carried out by a sound wave may then lead to a sign change of Γ and consequently different parts of the wave may correspond to different signs of Γ . As shown by Cramer & Kluwick (1984) new phenomena having no counterpart in the classical theory can arise. Examples include the partial disintegration of both compression and expansion shocks, collisions between compression and expansion shocks and the formation of sonic shocks having a speed identically equal to the convected sound speed immediately upstream or downstream of the front.

It has been pointed out earlier that the type of shock capable of propagating in any particular fluid is determined by the sign of the fundamental derivative. In addition, $|\Gamma|$ serves as a measure which characterizes the importance of nonlinear effects.

Specifically, the propagation distance over which the profile of a sound wave is distorted significantly is found to be proportional to $1/|\Gamma|$. Therefore if the unperturbed state of the fluid is close to the $\Gamma = 0$ line, as has been assumed in the investigation by Cramer & Kluwick (1984), nonlinear effects will need much larger propagation distances and times to come into play than in classical theory. As a result, the evolution of a sound wave in a medium having mixed nonlinearity $|\Gamma| \ll 1$ is expected to be very sensitive to deviations from the homogeneous state of the initially quiescent fluid on two grounds. First, even small gradients of the field quantities present in the unperturbed state may accumulate to give significant irregularities since the propagation distance required for the occurrence of nonlinear effects is so long. Second, if the unperturbed state is close to the $\Gamma = 0$ line even small changes of the thermodynamic state are associated with large relative changes of Γ .

It seems to be important, therefore, to assess in what respect the evolution of a wave in a stratified medium may differ from the behaviour of a wave propagating into a homogeneous medium. This is the aim of the present study, which shows that stratification effects may not only cause quantitative but can even lead to the occurrence of qualitatively new phenomena.

2. Transport equation

The transport equation which governs the propagation of small acoustic disturbances in a stratified medium can be derived in several ways. For example, Sen & Cramer (1987) have shown how propagation phenomena having mixed nonlinearity can be investigated using the method of multiple scales. Here we use a less formal approach which avoids the tedious calculation of the (already known) nonlinear terms and concentrate on the evaluation of the additional stratification effect. To this end, following earlier work by Bremmer (1951), the continuously stratified unperturbed medium is replaced by a set of homogeneous layers $0 < x < x_1$, $x_1 < x < x_2$, The approach is then similar to that developed by Mortell & Seymour (1976) for small-amplitude nonlinear disturbances in elastic composites. It is convenient first to introduce the non-dimensional quantities

$$u = \frac{\tilde{u}}{\tilde{a}_{10}}, \quad a = \frac{\tilde{a}}{\tilde{a}_{10}}, \quad \rho = \frac{\tilde{\rho}}{\tilde{\rho}_{10}}, \quad p = \frac{\tilde{p} - \tilde{p}_{10}}{\tilde{\rho}_{10} \tilde{a}_{10}^2}, \quad s = \frac{\tilde{s} - \tilde{s}_{10}}{\tilde{c}_{v10}}, \quad x = \frac{\tilde{x}}{\tilde{L}}, \quad t = \frac{\tilde{a}_{10} \tilde{t}}{\tilde{L}} \quad (2.1)$$

where \tilde{u} , $\tilde{\rho}$, \tilde{p} , \tilde{a} , \tilde{s} , \tilde{x} , \tilde{t} , \tilde{c}_v and \tilde{L} denote the velocity, the density, the pressure, the speed of sound, the entropy, the distance in the propagation direction, the time, specific heat at constant volume and the characteristic wavelength. Subscript 10 refers to the unperturbed state in the first layer.

In each layer asymptotic expansions of the form

$$\left. \begin{aligned} u_n &= \epsilon u_{n1} + \epsilon^2 u_{n2} + o(\epsilon^2), \\ \rho_n &= \rho_{n0} + \epsilon \rho_{n1} + \epsilon^2 \rho_{n2} + o(\epsilon^2), \\ p &= \epsilon p_1 + \epsilon^2 p_2 + o(\epsilon^2) \end{aligned} \right\} \quad (2.2)$$

are assumed to hold. Here $\rho_{n0} = \tilde{\rho}_{n0}/\tilde{\rho}_{10}$ and $\epsilon (\ll 1)$ is a measure of the small wave amplitude. Using the results obtained by Cramer & Kluwick (1984) the speed of the wave in each of the layers can be written as

$$\frac{dx}{dt} = a_{n0} + \epsilon^2 \left(\hat{\Gamma}_n + \frac{A_{n0}}{2a_{n0}} u_{n1} \right) u_{n1} + o(\epsilon^2), \quad (2.3)$$

where
$$\hat{\Gamma}_{n0} = \frac{1}{\epsilon} \Gamma_{n0} = O(1) \quad (2.4)$$

$$A_{n0} = \frac{\tilde{\rho}_{n0}^2}{\tilde{a}_{n0}} \tilde{\Lambda}_{n0} = O(1) \quad (2.5)$$

and
$$\tilde{\Lambda} = \frac{\partial}{\partial \tilde{\rho}} \left(\frac{\tilde{a}}{\tilde{\rho}} \Gamma \right) \Big|_s. \quad (2.6)$$

To determine the travel time of an acoustic signal emanating from layer 1 to layer n , say, we consider first the behaviour of the wave at a single contact discontinuity. Since we are interested in the local properties of the wave, e.g. the transmitted and reflected part of the incoming amplitude only, it is sufficient to solve the linearized version of the governing equations, which leads to the well-known result:

$$u_{m+1,1} i_{m+1,0} = u_{m,1} i_{m,0}, \quad i_{m,0} = (\rho_{m0} a_{m0})^{\frac{1}{2}}. \quad (2.7)$$

Combination of (2.3) and (2.7) then immediately yields the transport equation which governs the evolution of disturbances in a continuously stratified medium:

$$u_1 i_0(\sigma) = \text{constant} \quad \text{on} \quad \frac{dx}{dt} = a_0(\sigma) + \epsilon^2 \left(\hat{\Gamma}_0(\sigma) + \frac{A_0(\sigma)}{2a_0(\sigma)} u_1 \right) u_1. \quad (2.8)$$

Here it has been assumed that the unperturbed field quantities depend on the stretched coordinate

$$\sigma = \epsilon^2 x \quad (2.9)$$

rather than on x in order to ensure that nonlinear effects occurring in a homogenous medium and the effects due to stratification are of equal importance and thus lead to a significant distortion of the wave profile over propagation distances of $O(1/\epsilon^2)$.

Introducing the characteristic time variable

$$\bar{t} = t - \frac{1}{\epsilon^2} \int_0^\sigma \frac{d\bar{\sigma}}{a_0(\bar{\sigma})}, \quad (2.10)$$

(2.8) can be reduced to the relationship

$$\frac{\partial(i_0 u_1)}{\partial \sigma} - \frac{1}{a_0^2(\sigma)} \left(\hat{\Gamma}_0(\sigma) + \frac{A_0(\sigma)}{2a_0(\sigma)} u_1 \right) u_1 \frac{\partial(i_0 u_1)}{\partial \bar{t}} = 0. \quad (2.11)$$

Similar to the case of classical gas dynamics (see Gubkin 1958; Hayes, Haefeli & Kulsrud 1969) the results developed here for a temperature stratification can easily be generalized to include the effects of an additional pressure variation. The main difference will be the inclusion of a zeroth-order term for the pressure in (2.2). However, the transport equation for the disturbances will remain unchanged. These results are completely consistent with the WKB approximation.

Equation (2.11) has to be solved if $\hat{\Gamma}_0$ as well as A_0/a_0 and i_0 exhibit changes of $O(1)$ in the propagation direction. Inspection of figure 1, however, indicates that such a situation will be the exception rather than the rule since the thickness of the transition region, where the basic assumption $\Gamma = O(\epsilon)$ holds, is small ($O(\epsilon)$). In general than the variation of the field quantities inside the stratified medium will be associated with the small changes of the thermodynamic state given by

$$\left. \begin{aligned} |\hat{\Gamma}_0(\sigma) - \hat{\Gamma}_0(0)| &= O(1), & |A_0(\sigma) - A_0(0)| &= O(\epsilon), \\ |a_0(\sigma) - a_0(0)| &= O(\epsilon), & |i_0(\sigma) - i_0(0)| &= O(\epsilon). \end{aligned} \right\} \quad (2.12)$$

To the order of approximation considered here the dependence of A_0 , a_0 and i_0 on σ can then be neglected in (2.11):

$$\frac{\partial u_1}{\partial \sigma} - \frac{1}{a_0^2(0)} \left(\hat{\Gamma}_0(\sigma) + \frac{A_0(0)}{2a_0(0)} u_1 \right) u_1 \frac{\partial u_1}{\partial \hat{t}} = 0. \tag{2.13}$$

To eliminate the constants $A_0(0)$ and $a_0(0)$ we define the stretched quantities

$$\hat{t} = \frac{a_0(0) A_0(0)}{\hat{\Gamma}_0^2(0)} \hat{t}, \quad \hat{u} = \frac{A_0(0)}{a_0(0) \hat{\Gamma}_0(0)} u_1, \quad \hat{\Gamma} = \frac{\hat{\Gamma}_0(\sigma)}{\hat{\Gamma}_0(0)} \tag{2.14}$$

and finally obtain

$$\frac{\partial \hat{u}}{\partial \sigma} - (\hat{\Gamma}(\sigma) + \frac{1}{2} \hat{u}) \hat{u} \frac{\partial \hat{u}}{\partial \hat{t}} = 0. \tag{2.15}$$

Although (2.11) is slightly more general and more complicated than (2.15), the solutions are expected to be qualitatively similar. In the following we shall concentrate, therefore, on the discussion of solutions to (2.15). Specifically, we shall consider the boundary-value problem

$$\sigma = \sigma_0: \quad \hat{u} = U(\hat{t}). \tag{2.16}$$

A formal solution to (2.15) satisfying (2.16) is given by

$$\hat{u} = U(\xi), \quad \hat{t} = \xi - U(\xi) \int_{\sigma_0}^{\sigma} \hat{\Gamma}(\bar{\sigma}) d\bar{\sigma} - \frac{1}{2} U^2(\xi) (\sigma - \sigma_0). \tag{2.17}$$

Owing to the dependence of the wave propagation speed on the wave amplitude, however, this formal solution will in general cease to predict a unique relationship between (σ, \hat{t}) and \hat{u} if σ exceeds a critical value σ_s . In order to re-establish uniqueness, shock discontinuities have to be inserted into the wave profiles for $\sigma > \sigma_s$ by cutting off lobes of equal area. Since the description of such discontinuities involves the local values of the flow quantities immediately upstream and downstream of the front only, the results holding for shocks propagating into an initially homogeneous medium can be incorporated unchanged into a study of stratification effects. In particular, the expression for the propagation speed of weak shocks can be written in the form

$$\hat{a}_s^{-1} = \frac{1}{2} \hat{\Gamma}(\sigma) \frac{[\hat{u}^2]}{[\hat{u}]} + \frac{1}{6} \frac{[\hat{u}^3]}{[\hat{u}]}, \tag{2.18}$$

where the brackets denote jumps, i.e. $[Q] = Q_a - Q_b$ and the subscripts a and b refer to conditions after and before the shock.

Furthermore, the entropy change across shock fronts is given by

$$[\hat{s}] = \frac{\hat{\alpha}_0^2}{6 \hat{T}_0} \frac{[\hat{\rho}]^3}{\hat{\rho}_0^3} \left\{ \hat{\Gamma}_0 + \frac{1}{2} A_0 \left(\frac{\hat{\rho}_b - \hat{\rho}_0}{\hat{\rho}_0} - \frac{\hat{\rho}_a - \hat{\rho}_0}{\hat{\rho}_0} \right) + O \left(\frac{\hat{\rho} - \hat{\rho}_0}{\hat{\rho}_0} \right)^4 \right\}. \tag{2.19}$$

As in the case of homogeneous media, the requirement $[\hat{s}] \geq 0$ following from the second law of thermodynamics is too weak to rule out the formation of inadmissible shocks which violate the wave-speed ordering requirements that waves may merge with the front at arbitrary speeds but must not emanate from the front with a speed which differs from the shock speed. Shocks of the latter type having sonic conditions either upstream ($A_0 > 0$) or downstream ($A_0 < 0$) of the front are termed sonic shocks and they represent one source for the richness of unusual phenomena associated with the propagation of waves exhibiting mixed nonlinearity. For further details the reader is referred to the original study by Cramer & Kluwick (1984).

3. Qualitative behaviour of solutions to the transport equation

In general, (2.15) subject to appropriate boundary conditions has to be solved numerically. Before turning to the discussion of results for a wave pulse it is useful, however, to investigate briefly some aspects of the qualitative properties of such solutions and to illustrate these with applications to single velocity jumps. To this end (2.15) is recast in conservation form:

$$\frac{\partial \hat{u}}{\partial \sigma} + \frac{\partial \hat{j}}{\partial \hat{t}} = 0, \tag{3.1}$$

$$\hat{j} = -\left(\frac{1}{2}\hat{\Gamma}(\sigma)\hat{u}^2 + \frac{1}{6}\hat{u}^3\right), \tag{3.2}$$

where the flux \hat{j} and the scaled wavespeed \hat{v}_w satisfy the relationship

$$\hat{v}_w^{-1} = \left. \frac{\partial \hat{j}}{\partial \hat{u}} \right|_{\sigma}. \tag{3.3}$$

Furthermore, comparison of (2.18) and (3.2) shows that the speed \hat{a}_s of a shock discontinuity is given by

$$\hat{a}_s^{-1} = \left. \frac{[\hat{j}]}{[\hat{u}]} \right|_{\sigma}. \tag{3.4}$$

In figure 2 plots of \hat{j} versus \hat{u} are displayed for various values of $\hat{\Gamma}(0)$. It is seen, for example, that \hat{v}_w^{-1} increases (decreases) if $\hat{\Gamma}$ increases with the propagation distance provided \hat{u} is negative (positive). As in the case of a wave propagating into an initially homogeneous medium, the dependence of the wave speed on the magnitude of the disturbance carried by the wave will, in general, lead to the formation of shock discontinuities. By means of standard methods one finds that the shock formation distance σ_s satisfies the relationship

$$\sigma_s = \min \sigma_c, \tag{3.5}$$

where $\sigma_c(\xi)$ is the solution of

$$1 = \hat{u}'(\xi) \left[\int_{\sigma_0}^{\sigma_c} \hat{\Gamma}(s) ds + \hat{u}(\xi)(\sigma_c - \sigma_0) \right].$$

In contrast to the case of an initially homogeneous medium, however, stratification effects may also lead to the disintegration of an already existing shock front. This can be seen most easily by adopting the assumption that $\tilde{\Gamma}$ varies linearly with the propagation distance

$$\hat{\Gamma} = \hat{\Gamma}_0 + K(\sigma - \sigma_0). \tag{3.6}$$

For simplicity, let us consider first the limit $A_0 \rightarrow 0$. Equation (2.14) then yields $\tilde{u} \rightarrow 0$ and (3.2) can approximately be replaced by the relationship

$$\hat{j} = -\frac{1}{2}\hat{\Gamma}(\sigma)\hat{u}^2 + o(\hat{u}^2).$$

Accordingly, the location of wavelets $\xi = \text{const.}$ in the (σ, \hat{t}) -plane is determined from

$$\hat{t} = \xi - \hat{u}(\xi) \left[\hat{\Gamma}_0(\sigma - \sigma_0) + \frac{1}{2}K(\sigma - \sigma_0)^2 \right]. \tag{2.7}$$

Here the parameterization

$$\sigma = \sigma_0: \quad \hat{t} = \xi \tag{3.8}$$

has been imposed without loss of generality.

Inspection of the jump relationship (3.4) shows that the bisector rule

$$\hat{a}_s^{-1} = \frac{1}{2}(\hat{v}_{w,a}^{-1} + \hat{v}_{w,b}^{-1}) \tag{3.9}$$

is recovered in the limit $A_0 \rightarrow 0$.

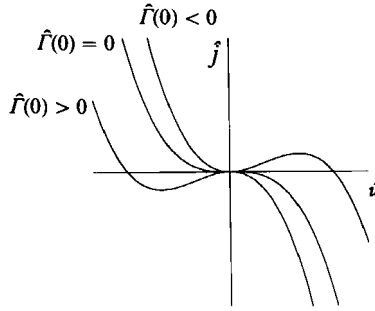


FIGURE 2. Plot of \hat{j} versus \hat{u} for various values of $\hat{\Gamma}(0)$.

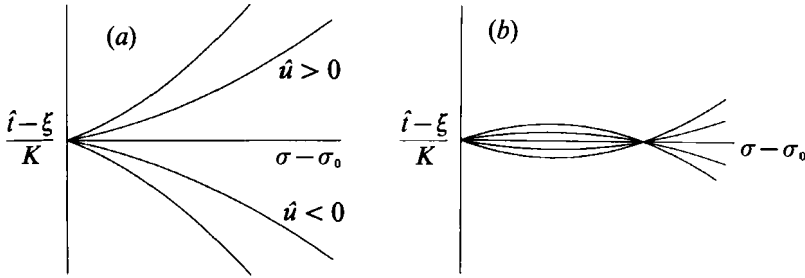


FIGURE 3. Characteristic curves for (a) $\hat{\Gamma}_0/K > 0$, (b) $\hat{\Gamma}_0/K < 0$.

It is convenient to rewrite (3.7) in the form

$$\hat{t} - \xi = \frac{\hat{\Gamma}_0^2}{2K} \hat{u}(\xi) - \frac{1}{2} K \hat{u}(\xi) (\sigma - \sigma_*)^2, \quad \sigma_* = \sigma_0 - \frac{\hat{\Gamma}_0}{K} \tag{3.10}$$

from which the properties of characteristic curves in stratified media having $\hat{\Gamma}_0/K > 0$ or $\hat{\Gamma}_0/K < 0$ can be inferred immediately. In the first case, figure 3(a), the sign of $\hat{\Gamma}$ in the unperturbed state does not change with the propagation distance. As a consequence the speed \hat{v}_w of a wavelet carrying constant values of \hat{u} is either positive or negative for all values of $\sigma \geq \sigma_0$, indicating that the wave pattern associated with a boundary-value problem will be qualitatively similar to that obtained if $\hat{\Gamma}$ is constant. However, if $\hat{\Gamma}_0/K < 0$, figure 3(b), the local values of $\hat{\Gamma}$ and \hat{v}_w^{-1} vanish at $\sigma = \sigma_* > \sigma_0$ thus leading to new phenomena. Specifically, evaluation of (3.10) yields the result that all characteristic curves $\xi = \text{const.}$ pass through the point

$$\hat{t} - \xi = 0, \quad \sigma = 2\sigma_* - \sigma_0. \tag{3.11}$$

As an application of (3.9), (3.10), (3.11) let us calculate the evolution of a single velocity step

$$\sigma = \sigma_0: \quad \begin{cases} u = \hat{u}_0 & \hat{t} > 0 \\ \hat{u} = 0 & \hat{t} \leq 0. \end{cases} \tag{3.12}$$

As expected, the resulting wave pattern in the (σ, \hat{t}) -plane qualitatively resembles that of the $\hat{\Gamma}$ -constant case provided $\hat{\Gamma}_0/K > 0$: the imposed velocity jump immediately disintegrates into a wave fan

$$\hat{t} = -\hat{u}[\hat{\Gamma}_0(\sigma - \sigma_0) + \frac{1}{2}K(\sigma - \sigma_0)^2], \quad 0 \leq |\hat{u}| \leq |\hat{u}_0| \tag{3.13}$$

if $\hat{\Gamma}_0 \geq 0$ and $\hat{u}_0 \leq 0$ (figure 4a), while a shock forms if $\hat{\Gamma}_0 \geq 0$ and $\hat{u}_0 \geq 0$ (figure 4b).

A completely different behaviour is observed if $\hat{\Gamma}_0/K < 0$. Results for $\hat{\Gamma}_0 \geq 0$ and $\hat{u}_0 \leq 0$ are depicted in figure 4(c). In agreement with the wave pattern shown in figure

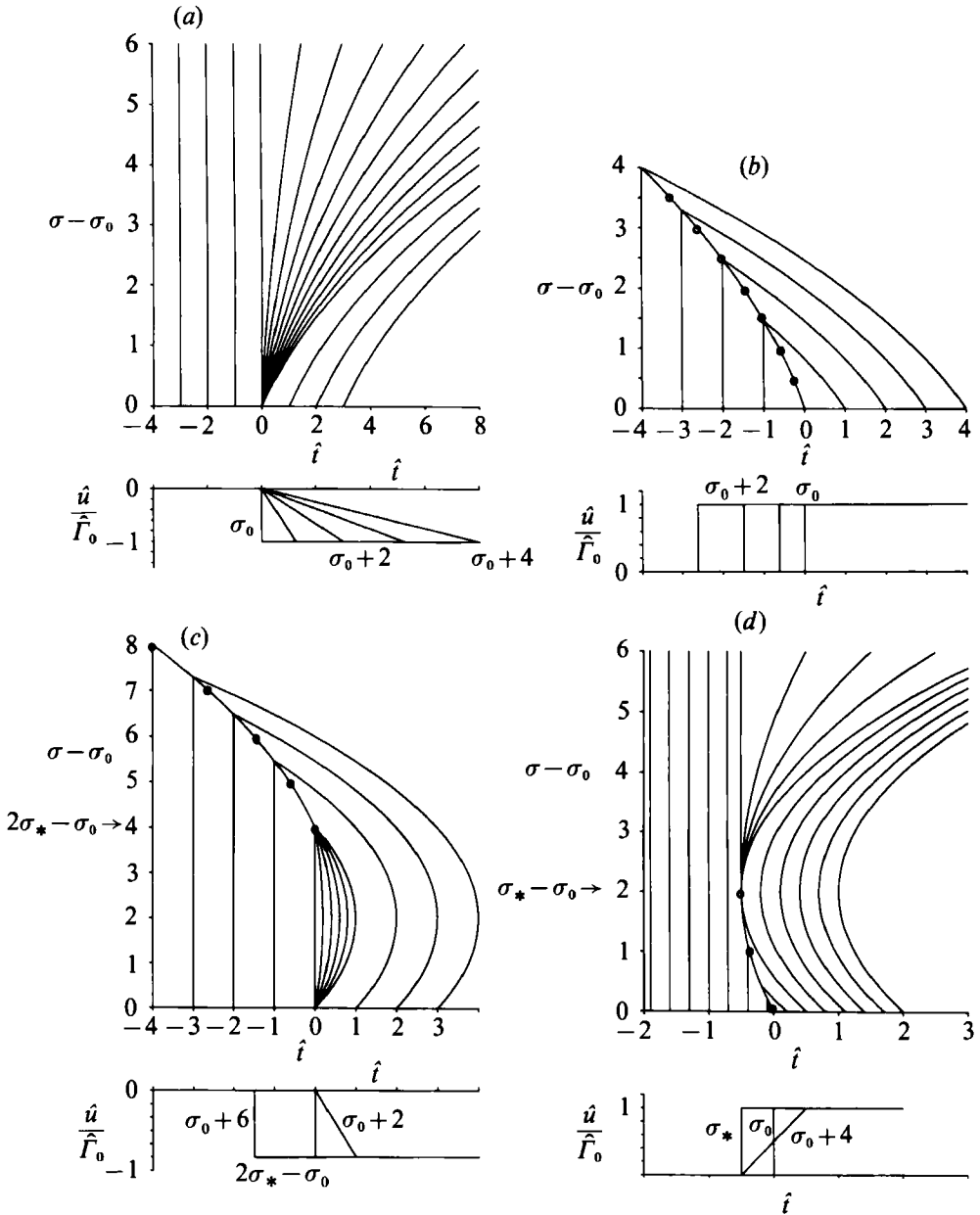


FIGURE 4. (a) Wave fan evolution for $\hat{F}_0 \geq 0$, $\hat{u}_0 \leq 0$ and (b) shock wave evolution for $\hat{F}_0 \geq 0$, $\hat{u}_0 \geq 0$: $\hat{F}_0/K > 0$ ($\hat{F}_0 = 1.0$, $K = 0.5$). (c) Wave evolution for $\hat{F}_0 \geq 0$, $\hat{u}_0 \leq 0$ (wave fan focuses at $\sigma_s = 2\sigma_* - \sigma_0$) and (d) wave evolution for $\hat{F}_0 \geq 0$, $\hat{u}_0 \geq 0$ (sonic shock disintegrates at $\sigma = \sigma_*$): $\hat{F}_0/K < 0$ ($\hat{F}_0 = 1.0$, $K = -0.5$).

4(a) the imposed velocity jump leads to the occurrence of a wave fan initially. Once \hat{F} has changed sign, however, the characteristic curves forming this fan start to converge and they eventually focus at the point $\hat{t} = 0$, $\sigma = \sigma_s = 2\sigma_* - \sigma_0$. Furthermore, it is seen that the shape of the velocity profile imposed at $\sigma = \sigma_0$ is recovered at $\sigma = \sigma_s$. Owing to the changed sign of \hat{F} the associated jump $[\hat{u}] = \hat{u}_0$ produces a stable shock front propagating into the region $\sigma > \sigma_s$. Finally, if $\hat{F}_0 \geq 0$ and $\hat{u}_0 \geq 0$ a shock discontinuity is generated at $\sigma = \sigma_0$ (figure 4d), again in

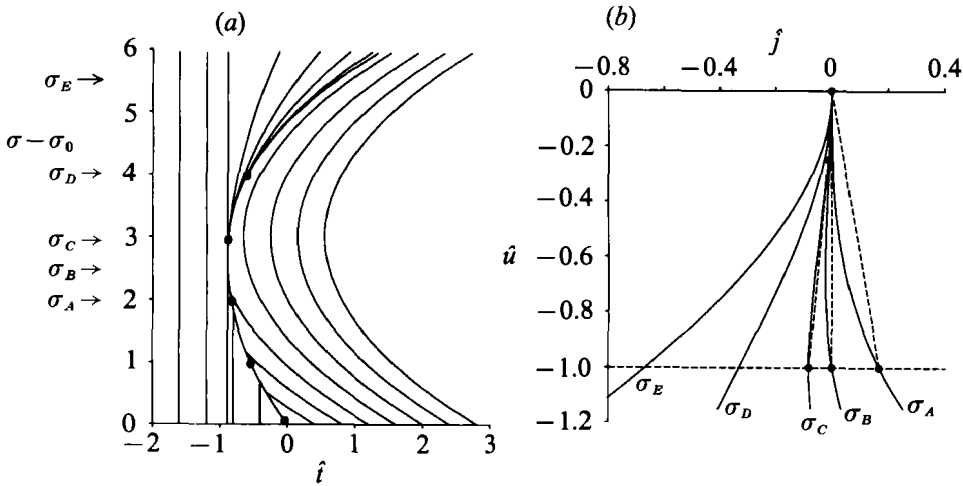


FIGURE 5. Characteristic curves of (2.15), (3.12) for $\hat{\Gamma}_0 < 0, K > 0, A_0 > 0, \hat{u}_0 < 0$. (b) Plot of j versus \hat{u} for various values of σ . Dotted line denotes the shock jump. (Results for $\hat{\Gamma}_0 = -1.0, K = 0.5$.)

agreement with the results holding for $\hat{\Gamma}_0/K > 0$ (figure 4b). Since $|\hat{\Gamma}|$ decreases with increasing propagation distance, the motion of the shock front whose position is determined by (3.9) slows down despite the fact that the shock strength remains unchanged and sonic conditions are reached at $\sigma = \sigma_*$. For $\sigma > \sigma_*$ velocity jumps characterized by $[\hat{u}]/\hat{\Gamma}_0 > 0$ no longer represent admissible shock discontinuities and, consequently, the sonic shock front at $\sigma = \sigma_*$ disintegrates into a wave fan, given by

$$\hat{t} = \frac{\hat{u}_0 \hat{\Gamma}_0^2}{4K} - \frac{1}{2} K \hat{u} (\sigma - \sigma_*)^2, \quad 0 \leq |\hat{u}| \leq |\hat{u}_0|. \tag{3.14}$$

The fact that shocks may terminate at a finite distance from their origin was pointed out first by Kluwick & Czemetschka (1990) who studied the evolution of spherical and cylindrical waves having mixed nonlinearity which propagate into a homogeneous medium. It is a characteristic feature of this phenomenon that the shock strength decreases continuously to zero. In contrast, the present analysis has shown that stratification effects may cause a shock of finite strength to disappear suddenly at a point where the local value of $\hat{\Gamma}$ vanishes if $A_0 = 0$.

It is a well-known result of classical gas dynamics that the strength of a shock can vanish only in the limit of infinite time and infinite distance. That this is not necessarily true if one considers waves having mixed nonlinearity rests on the existence of sonic shock conditions. If $A_0 = 0$ sonic shock conditions require $\hat{\Gamma} = 0$ immediately before the front and, consequently, shocks can terminate at the $\hat{\Gamma} = 0$ locus only. If $A_0 \neq 0$, however, sonic shocks can exist over a whole range of upstream conditions, which in turn leads to a modification of the shock termination phenomenon as sketched in figure 5(a, b), adopting again boundary conditions (2.12). Specifically it has been assumed that $\hat{\Gamma}_0 < 0, K > 0, A_0 > 0$ and $\hat{u}_0 < 0$. Figure 5(a) then displays the resulting wave pattern while figure 5(b) indicates the properties of the shock front at various distances from the boundary $\sigma = \sigma_0$ in the (j, \hat{u}) -plane.

At $\sigma = \sigma_0$ the imposed velocity step leads to the formation of a stable expansion shock $[\hat{u}] = \hat{u}_0 < 0$. As the shock front propagates to the left $|\hat{\Gamma}|$ decreases and vanishes at $\sigma = \sigma_A$. In contrast to the case $A_0 = 0$, however, the strength of the shock remains unchanged as it passes through the $\hat{\Gamma} = 0$ locus $\sigma = \sigma_B$ and eventually

reaches sonic conditions at $\sigma = \sigma_c$. Owing to the requirement that the shock must satisfy sonic upstream conditions as it propagates further, a precursor region forms for $\sigma > \sigma_c$. Inside this precursor region the shock strength decays and finally vanishes at $\sigma = \sigma_D$. Here the value of $\hat{u} = \hat{u}_0$ immediately downstream of the front must agree with the value of \hat{u} at the inflexion point of the corresponding \hat{j} versus \hat{u} plot. This condition determines the local value of $\hat{\Gamma}$ at the shock termination point and $\sigma = \sigma_D$ is given by

$$\hat{\Gamma} = -u_0: \quad \sigma_D - \sigma_0 = -\frac{\hat{\Gamma}_0 + \hat{u}_0}{K}. \quad (3.15)$$

In the limit $A_0 \rightarrow 0$ ($\hat{u}_0 \rightarrow 0$) the interval $[\sigma_c, \sigma_D]$ shrinks to a single point $\sigma = \sigma_*$ and the flow pattern shown in figure 4(d) is recovered.

In order to conclude this brief discussion of the evolution of single velocity jumps we consider next the boundary-value problem

$$\sigma = \sigma_0: \quad \begin{cases} \hat{u} = 0, & t > 0 \\ \hat{u} = \hat{u}_0, & t \leq 0. \end{cases} \quad (3.16)$$

It is easily seen that the solution to this problem for $A_0 = 0$ is obtained from the solution subject to the boundary conditions (3.12) if \hat{t} is replaced by $-\hat{t}$. As a typical example of the case $A_0 \neq 0$, figure 6 summarizes the flow properties assuming $\hat{\Gamma}_0 < 0$, $K > 0$, $A_0 > 0$ and $\hat{u}_0 > 0$. As in figure 5 a stable expansion shock $[\hat{u}] = -\hat{u}_0$ is generated at $\sigma = \sigma_0$. With increasing propagation distance the difference between the shock speed and the speed of the wavelets merging from behind the front decreases and sonic downstream conditions are reached at $\sigma = \sigma_A$ where the local value of $\hat{\Gamma}$ is still negative. While the shock strength has remained constant up to $\sigma = \sigma_A$ the shock weakens as σ increases further and it vanishes at

$$\sigma = \sigma_c: \quad \hat{\Gamma}(\sigma_c) = 0.$$

It has been pointed out already that solutions to the transport equation have in general to be calculated numerically. If the boundary conditions are sufficiently simple as in the cases (3.12) and (3.16), however, analytical results including expressions for the location of shock fronts can be obtained. To this end it is convenient to introduce the scaled stream function $\hat{\psi}$

$$\frac{\partial \hat{\psi}}{\partial \hat{t}} = \hat{u}, \quad \frac{\partial \hat{\psi}}{\partial \sigma} = -\hat{j}. \quad (3.17)$$

Insertion into the jump relationships immediately leads to the result that $[\hat{\psi}]$ does not vary along a shock front, and without loss of generality we require that $\hat{\psi}$ is continuous across such a front. The position of a shock in the (σ, t) -plane is then determined by the relationship

$$[\hat{\psi}(\sigma, \hat{t})] = 0. \quad (3.18)$$

To evaluate (3.18) we first calculate the derivative of $\hat{\psi}$ with respect to σ along a characteristic curve $\xi = \text{constant}$:

$$\left. \frac{\partial \hat{\psi}}{\partial \sigma} \right|_{\xi} = \frac{\partial \hat{\psi}}{\partial \sigma}(\sigma, \hat{t}) + \frac{1}{v_w} \frac{\partial \hat{\psi}}{\partial \hat{t}}(\sigma, \hat{t}) = -\frac{1}{2} \hat{\Gamma}(\sigma) \hat{u}^2 - \frac{1}{3} \hat{u}^3. \quad (3.19)$$

Integration, taking into account the parametrization (3.8) and introducing the notation of an F -function:

$$\hat{u} = F'(\xi), \quad (\prime = d/d\xi) \quad (3.20)$$

yields

$$\hat{\psi}(\xi, \sigma) = F(\xi) - \frac{1}{2} F'^2(\xi) \int_{\sigma_0}^{\sigma} \hat{\Gamma}(s) ds - \frac{1}{3} F'^3(\xi) (\sigma - \sigma_0). \quad (3.21)$$

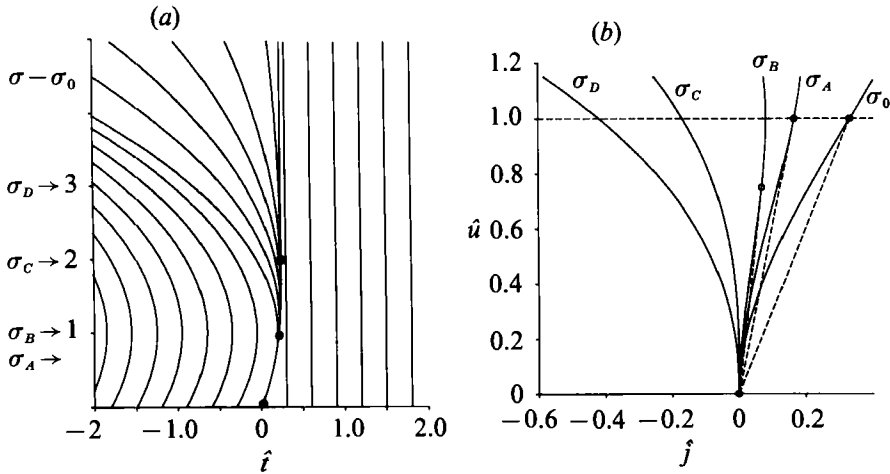


FIGURE 6. (a) Characteristic curves of (2.15), (3.16) for $\hat{T}_0 < 0$, $K > 0$, $A_0 > 0$ and $\hat{u}_0 > 0$. (b) Plot of j versus \hat{u} for various values of σ . Dotted line denotes the shock jump. (Results of $\hat{T}_0 = -1.0$, $K = 0.5$.)

In principle, ξ can be eliminated from this relationship by means of (2.17)

$$\hat{t} = \xi - F'(\xi) \int_{\sigma_0}^{\sigma} \hat{T}(s) ds - \frac{1}{2} F'^2(\xi) (\sigma - \sigma_0). \tag{3.22}$$

In general, however, it is more convenient to represent the shock curve in parametric form

$$[\hat{\psi}(\xi, \sigma)] = 0, \quad [\hat{t}(\xi, \sigma)] = 0 \tag{3.23}$$

rather than to apply (3.19).

Equations (3.21) and (3.22) are based on the assumption that both characteristic curves that merge in a point of the shock front originate at the boundary $\sigma = \sigma_0$. They therefore fail if wavelets emanate from the shock front itself, e.g. if sonic conditions are reached before or behind the jump discontinuity. As in the case of constant \hat{T} investigated by Kluwick & Koller (1988) it is possible to derive an ordinary differential equation which governs the propagation of sonic shock fronts.

Equations (3.21), (3.22), and (3.23) simplify considerably if $\hat{u} \equiv 0$ either before or after the shock and if the shock strength is constant, $[\hat{u}] = \hat{u}_0$. As a consequence $F(\xi) = \hat{u}_0 \xi$ and the location of the shock in the (σ, \hat{t}) -plane is given by

$$\hat{t} = -\frac{1}{2} \hat{u}_0 \int_{\sigma_0}^{\sigma} \hat{T}(s) ds - \frac{1}{6} \hat{u}_0^2 (\sigma - \sigma_0). \tag{3.24}$$

Adopting the assumption (3.6) that \hat{T} varies linearly with the propagation distance one finds

$$\hat{t} = -\frac{1}{2} \hat{u}_0 \{ (\hat{T} + \frac{1}{3} \hat{u}_0) (\sigma - \sigma_0) + \frac{1}{2} K (\sigma - \sigma_0) \}. \tag{3.25}$$

4. Numerical solutions

The quantitative results of § 3 are illustrated by application to the boundary-value problem

$$\sigma = \sigma_0: \begin{cases} \hat{u} = 0 & \hat{t} > 1 \\ \hat{u} = \hat{u}_0, & 0 \leq \hat{t} \leq 1 \\ \hat{u} = 0, & \hat{t} < 0. \end{cases} \tag{4.1}$$

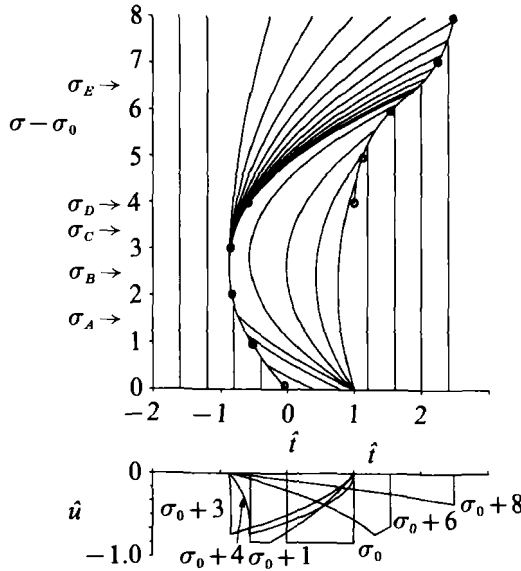


FIGURE 7. Wave evolution for $\hat{u}_0 = -1.0$, $\hat{F}_0 = -1.0$, $K = 0.5$.

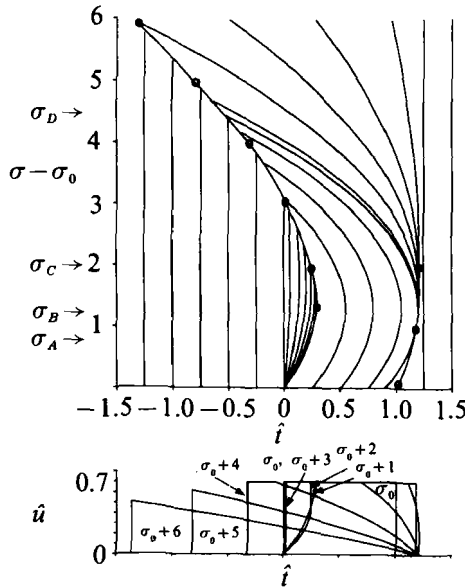


FIGURE 8. Wave evolution for $\hat{u}_0 = 0.7$, $\hat{F}_0 = -1.0$, $K = 0.5$.

The solution to (2.15) subject to (4.1) is constructed for \hat{F} given by (3.6) with $\hat{F}_0 < 0$, $K > 0$.

When $\hat{u}_0 < 0$ the wave behaviour is shown in figure 7. The initial evolution involves a stable expansion shock (see figure 5) and a compression fan. The fan originating at $\hat{i} = 1$ reaches the expansion shock at $\sigma = \sigma_A$, resulting in a decay of the shock strength for $\sigma > \sigma_A$. When $\sigma = \sigma_B$ the expansion shock satisfies sonic conditions and a precursor region forms. The velocity of the shock slows down and the strength of the shock decays and vanishes at $\sigma = \sigma_C$. In the compression fan the characteristic curves begin to converge as \hat{F} changes sign and becomes positive. This leads to the

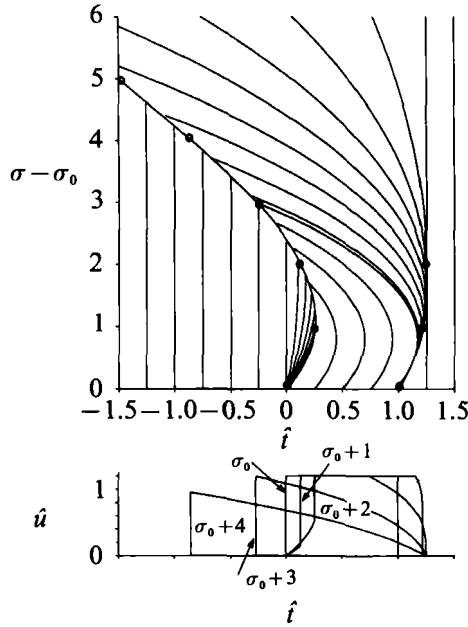


FIGURE 9. Wave evolution for $\hat{u}_0 = 1.2$, $\hat{I}_0 = -1.0$, $K = 0.5$.

formation of a stable compression shock at $\sigma = \sigma_D = 2\sigma_* - \sigma_0$ which propagates with increasing strength until interaction with characteristics from the precursor region occurs at $\sigma = \sigma_E$. The final shock–fan interaction causes the shock to slow down and decay in strength, ultimately resulting in a sawtooth wave structure.

When $0 < \hat{u}_0 < 1$ the behaviour of the wave is similar to that of $\hat{u}_0 < 0$ and is illustrated in figure 8. A stable expansion shock (see figure 6) and a compressive wave fan evolve from $\sigma = \sigma_0$. The expansion fan arises from the disintegration of the initial velocity jump at $\hat{t} = 0$. As $|\hat{I}|$ decreases, the shock slows down and becomes sonic at $\sigma = \sigma_A$ with a precursor region forming for $\sigma \geq \sigma_A$. The shock strength which was constant up to $\sigma = \sigma_A$ weakens and eventually vanishes at $\sigma = \sigma_C$. As \hat{I} increases and eventually changes sign at $\sigma = \sigma_0 - \hat{I}_0/K$, the characteristics for $\hat{u} = \hat{u}_0$ slow down and change direction in the (\hat{t}, σ) -plane. This leads to their intersection with characteristics in the wave fan for $\sigma > \sigma_B$, resulting in a compression shock. When all the characteristics for $\hat{u} = \hat{u}_0$ are absorbed into the trailing shock, the strength decays as characteristics from the precursor region enter the shock for $\sigma \geq \sigma_D$. Again the long-time behaviour is described by a sawtooth profile.

When $\hat{u}_0 > 1$ the velocity discontinuity at $\hat{t} = 0$ cannot propagate as a single fan as in the previous example. Requiring a smooth velocity transition from $\hat{u} = 0$ to $\hat{u} = \hat{u}_0$ involves a shock–fan combination, with a shock at $\sigma = \sigma_0$ of sonic strength. For $1.0 < \hat{u}_0 < 1.5$ the evolving signal is shown in figure 9 and is similar, with the exception of the initial development at $\hat{t} = 0$, to that shown in figure 8.

When $\hat{u} = 1.5$ the speed of the front shock equals the wave speed just before the shock. A consequence of this is that for $\hat{u}_0 > 1.5$ the initial discontinuity at $\sigma = 1$ cannot propagate as an isolated shock. There is immediate disintegration into a sonic shock–fan combination as seen in figure 10. The sonic shock then propagates as in previous examples.

The results illustrated in figures 5–10 involved combining the analysis results of §3 with, where necessary, numerical integration of the characteristic equations for

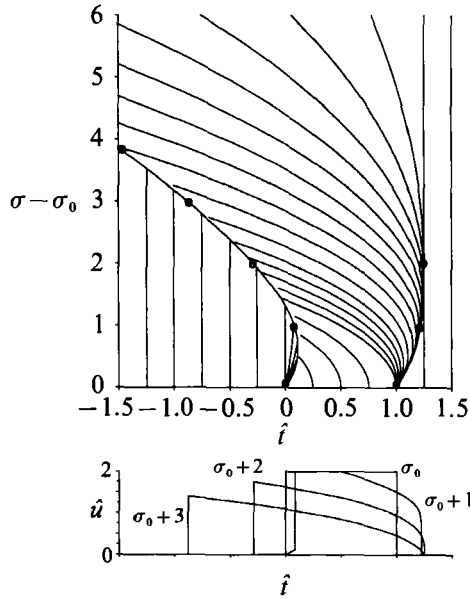


FIGURE 10. Wave evolution for $\hat{u}_0 = 2.0$, $\hat{\Gamma}_0 = -1.0$, $K = 0.5$.

(2.15). The shock paths were computed from the integration of (2.18). Integration was carried out using the numerical subroutine library IMSL and the ordinary differential equation solvers found therein.

5. Concluding remarks

The evolution equation for weakly nonlinear waves propagating into a fluid having mixed nonlinearity when the properties vary in the propagation direction has been derived. A discussion of its properties based on the method of characteristics indicates the occurrence of interesting new phenomena. Specifically it is found that shocks may terminate at a finite distance from their origin with either zero – or even more surprising – with finite strength. Moreover expansion/compression fans are seen to focus again to form shocks if they enter regions where the fundamental derivative $\hat{\Gamma}$ is negative/positive. These conclusions are confirmed by analytical solutions describing single steps as well as numerical solutions for square pulses which have been obtained for the case that $\hat{\Gamma}$ varies linearly with propagation distance.

Generalization of the present work currently in progress include studies dealing with viscous effects as well as effects which occur if the fluid is stratified parallel rather than normal to the propagation direction. In the latter case wave fronts will turn and it will be interesting to determine whether it is possible to keep the associated rays confined to a region where $\hat{\Gamma}$ is small. If so it should be possible to construct acoustic wave guides having much smaller losses than in the classical case.

Another type of wave front turning, caused by the variation of the wave amplitude rather than the variation of the unperturbed flow quantities, occurs if one considers very narrow acoustic beams. The appropriate form of the model equation which governs the evolution of weakly nonlinear disturbances inside such beams was derived first by Zabolotskaya & Khokhlov (1969, 1970) (adopting the assumption that the fluid is a perfect gas). Starting from a new family of symmetries to this so-

called Zabolotskaya–Khokhlov equation, Cates & Crighton (1990) were able to deduce a set of exact similarity solutions which sheds some light on nonlinear diffraction and caustic formation. Interesting new effects are expected to occur if the perfect gas is replaced by a dense gas having mixed nonlinearity.

REFERENCES

- BETHE, H. A. 1942 The theory of shock waves for an arbitrary equation of state. *Office Sci. Res. Dev. Rep.* 545.
- BORISOV, A. A., BORISOV, AL. A., KUTATELADZE, S. S. & NAKORYKOV, V. E. 1983 Rarefaction shock wave near the critical liquid–vapour point. *J. Fluid Mech.* **126**, 59–73.
- BREMMER, H. 1951 The WKB approximation as the first term of a geometrical-optical series. *Commun. Pure Appl. Maths* **4**, 105–115.
- CATES, A. T. & CRIGHTON, D. G. 1990 Nonlinear diffraction and caustic formation. *Proc. R. Soc. Lond. A* **430**, 69–88.
- CRAMER, M. S. 1991 Nonclassical dynamics of classical gases. In *Nonlinear Waves in Real Fluids*, (ed. A. Kluwick), pp. 91–145. Springer.
- CRAMER, M. S. & KLUWICK, A. 1984 On the propagation of waves exhibiting both positive and negative nonlinearity. *J. Fluid Mech.* **142**, 9–37.
- GUBKIN, K. E. 1958 Propagation of discontinuities in sound wave. *Prikl. Matem. Mekhan.* **22**, 561–564.
- HAYES, W. D. 1960 *Gasdynamic Discontinuities*. Princeton Series on High Speed Aerodynamics and Jet Propulsion. Princeton University Press.
- HAYES, W. D., HAEFELI, R. C. & KULSRUD, H. E. 1969 Sonic boom propagation in a stratified atmosphere, with computer program. *NASA CR-1299*.
- KLUWICK A. & CZEMETSCHKA, E. 1990 Kugel und Zylinderwellen in Medien mit positiver und negativer Nichtlinearitaet. *Z. Angew. Math. Mech.* **70** (4), T207–T208.
- KLUWICK, A. & KOLLER, F. 1988 Ausbreitung periodischer Wellen kleiner Amplitude in Gasen mit grossen spezifischen Waermen. *Z. Angew. Math. Mech.* **68** (4), T306–T307.
- MORTELL, M. P. & SEYMOUR, B. R. 1976 Wave propagation in a nonlinear laminated material: A derivation of geometric acoustics. *Q. J. Mech. Appl. Maths* **29**, 457–466.
- SEN, R. & CRAMER, M. S. 1987 A general Scheme for the derivation of evolution describing mixed nonlinearity. *VPI-E-87-16 Rep.*
- THOMPSON, P. A. & LAMBRAKIS, K. C. 1973 Negative shock waves. *J. Fluid Mech.* **60**, 187–208.
- ZABOLOTSKAYA, E. A. & KHOKHLOV, R. V. 1969 Quasi-plane waves in the nonlinear acoustics of confined rays. *Sov. Phys.-Acoust.* **15**, 35–40.
- ZABOLOTSKAYA, E. A. & KHOKHLOV, R. V. 1970 Convergent and divergent sound beams in nonlinear media. *Sov. Phys.-Acoust.* **16**, 39–42.
- ZEL'DOVICH, YA. B. 1946 On the possibility of rarefaction shock waves. *Zh. Eksp. Teor. Fiz.* **4**, 363–364.